GENE DELIVERY

ELSEVIER

siRNA-containing liposomes modified with polyarginine effectively silence the targeted gene

Chunling Zhang [a,1], Ning Tang [a,1], XingJun Liu [a,b], Wei Liang [a,*],
Wei Xu [a], Vladimir P. Torchilin [c]

[a] *National Laboratory of Biomacromolecules, Institute of Biophysics, Chinese Academy of Sciences, 15 Datun Road, Beijing 100101, China*
[b] *School of Pharmacy, Shenyang Pharmaceutical University, Shenyang 110016, China*
[c] *Department of Pharmaceutical Sciences, Northeastern University, MA 02115, USA*

Abstract

Development of RNA interference (RNAi) technology utilizing the short interfering RNA sequences (siRNA) based 'targeted' therapeutics has focused on creating methods for delivering siRNAs to cells and for enhancing siRNA stability in vitro and in vivo. Here, we describe a novel approach for siRNA cellular delivery using siRNA encapsulated into liposomes additionally bearing arginine octamer (R8) molecules attached to their outer surface (R8-liposomes). The R8-liposomal human double minute gene 2 (HDM2)-siRNA demonstrated a significant stability against degradation in the blood serum (siRNA-loaded R8-liposomes remained intact even after 24-h incubation), and higher transfection efficiency into all three tested lung tumor cell lines. siRNA delivery successfully proceeds in the presence of plasma proteins, and R8-liposomes demonstrate low non-specific toxicity. The mechanism of action of R8-liposome-encapsulated siRNA is associated with the RNAi-mediated degradation of the target mRNA. siRNA in R8-liposomes effectively inhibited the targeted gene and significantly reduced the proliferation of cancer cells. The approach offers the potential for siRNA delivery for various in vitro and in vivo applications.
© 2006 Elsevier B.V. All rights reserved.

Keywords: siRNA delivery; Liposomes; Polyarginine; HDM2 gene; Lung cancer

1. Introduction

RNAi is being exploited for a variety of laboratory applications in biology and as a promising therapeutic product [1]. The clinical use of siRNA is hindered by three major problems: (1) rapid enzymatic degradation resulting in a short half-life in the blood; (2) poor cellular uptake; (3) insufficient tissue bioavailability [2–4]. In general, these problems can be partly overcome by mixing siRNAs with cationic lipids or cationic polymers to form complexes, which could be additionally surface-modified with specific ligands allowing for targeting of required tissues [5]; or by modifying siRNAs with cell-penetrating peptides (CPPs), which have been successfully applied for the delivery of various cargoes into a variety of cells both in vitro and in vivo [6–9]. However, these approaches frequently failed because of aggregation of siRNA-carrying positively charged complexes in the blood in the presence of plasma proteins, which results in unfavorable pharmacokinetics mainly due to the rapid uptake into the tissues of the mononuclear phagocytic system (MPS) [10].

Lipoplexes, also known as cationic amphiphiles or cationic liposomes, have been developed that are capable of delivering DNA or RNA, including both plasmids encoding siRNA sequences and siRNAs, through the cellular membrane, and achieving high activity of the RNAi [11–13]. In particular, Lipofectamine2000 is frequently used for the delivery of siRNA [14,15]. Despite the certain success using Lipoplexes, these agents allow for little control over the process of their interaction with siRNA leading to the final product, siRNA-lipoplex particle, of excessive size, low stability, and with incomplete encapsulation of siRNA molecules, which thereby exposes siRNA to potential enzymatic or physical degradation prior to delivery to cells. The complexes are sensitive towards serum, and therefore, optimal transfection must be performed using

---

serum-free conditions, which has obvious shortcomings for potential in vivo applications. In addition, such complexes do not work efficiently with many cell types and are toxic to cells and experimental animals [16].

An alternative approach is to synthesize lipophilic derivatives of siRNA by coupling it with hydrophobic moieties, such as cholesterol, which significantly improves the in vitro cellular uptake and in vivo pharmacological properties of siRNAs [4,17].

Here, we describe the development of a new strategy for functional siRNA delivery to cells by loading siRNA into liposomes bearing arginine octamer molecules attached to the liposome surface (R8-liposomes). R8 belongs to a large group of so-called cell-penetrating peptides (CPP), which are positively charged and can enter cells when added exogenously [18]. Various CPPs have been successfully used for the delivery of exogenous molecules, such as oligonucleotides and proteins, and even small particles, such as iron oxide nanoparticles, liposomes, and quantum dots, into the cytoplasm and nuclei of cultured cells [6–9,19]. Thus, DNA-loaded liposomes were delivered into various cells by multiple TAT peptide molecules attached to the liposome surface and allowed for the successful transfection with TAT–liposome–DNA complexes both in vitro and in vivo [20]. Synthetic oligo-arginines, such as 9-mer and 8-mer (R8), were shown to be very effective CPPs [21] allowing, for example, for successful cell transfection with R8-luciferase-encoding plasmid complexes [22].

We hypothesized that siRNA-loaded R8-liposomes formulated using a charge neutral ratio of 1,2-dioleoyl-3-trimethylammonium-propane (DOTAP)/siRNA with the addition of the poly(ethylene glycol)-phosphatidylethanolamine (PEG-PE) conjugate for increased in vivo longevity, will provide an effective transfection system in vitro and in vivo.

2. Materials and methods

2.1. Materials

Egg phosphatidylcholine (egg PC), 1,2-dioleoyl-3-trimethylammonium-propane (DOTAP), cholesterol (Ch), 1,2-dipalmitoyl-sn-glycero-3-phosphoethanolamine (DPPE), distearoyl-sn-glycero-3-phosphoethanolamine-n-[methoxy (polyethyleneglycol)-2000] (PEG-PE), Lissamine rhodamine B-labeled glycerophosphoethanolamine (Rh-PE) were from Avanti Polar Lipids. Triethylamine, polyoxyethylene (MW 3400)-bis (p-nitrophenyl carbonate) [(pNP)$_2$-PEG)], CL-4B Sepharose, and components of buffer solutions were purchased from Sigma. Cell culture media and fetal bovine serum (FBS) were from GIBCO; Lipofectamine2000 was from Invitrogen. Water was deionized and then distilled. All solutions and buffer components were made from analytical grade chemicals.

2.2. siRNA synthesis

21 nt siRNAs were chemically synthesized as 2′-bis (acetoxythoxy)-methyl ether-protected oligos by Shanghai GenePharma Co. (Shanghai, China). Synthetic oligonucleotides were deprotected, annealed, and purified as described by the

manufacturer. Duplex formation was confirmed by 20% nondenaturing polyacrylamide gel electrophoresis. The siRNA samples were stored in diethylpyrocarbonate (DEPC)-treated water at −80 °C. The siRNA sequence targeting HDM2 (GenBank: Acc. no. NM_002392) corresponded to the coding regions 42–62 (5′-AACCACCTCACAGATTCCAGC-3′) after the starting codon, including: sense 5′-CCACCUCACA-GAUUCCAGCtt-3′, antisense 5′-GCUGGAAUCUGUGAG-GUGGtt-3′. To determine the uptake efficiency of siRNA, fluorescence-labeled siRNA was synthesized by coupling fluorescein isothiocyanate (FITC, purchased from Aldrich) to the 3′position of the sense strand to be used. The mock siRNA sequence was 5′-AAUAGUGUAUACGGCAUGCdTdT-3′.

2.3. Peptide synthesis

Polyarginine peptides were synthesized using solid phase techniques and commercially available fluorenylmethoxycarbonyl (Fmoc) amino acids, resins and reagents (PE Biosystems, CA) on an Applied Biosystems 433 peptide synthesizer. Fmoc chemistry was used with O-(7-azabenzotriazol-1-yl)-1,1,3,3-tetramethyluronium hexafluorphosphate (HATU) as coupling reagent. The peptides were cleaved from the resin using 96% trifluoroacetic acid, 2% triisopropyl silane and 2% phenol for 12 h. Subsequently, the peptides were filtered from the resin, precipitated with the diethyl ether, purified using HPLC reverse-phase columns (Alltech Altima, Chicago, IL, USA), and characterized using matrix-assisted laser desorption mass spectrometry (Perceptive Biosystems, Boston, MA, USA). In this study, arginine octamer (R8) was used as cell-penetrating peptide for siRNA delivery into cells.

2.4. pNP-PEG-PE synthesis

pNP-PEG-PE was synthesized according to previously reported method with some changes [23]. Briefly, 100 mg of DPPE was dissolved in chloroform to obtain a 50 mg/ml of solution. The solution was supplemented with 2 ml of TEA. Two grams of (pNP)$_2$-PEG dissolved in 20 ml of chloroform was added to the mixture, and the sample was incubated overnight at room temperature with stirring under argon. Then the organic solvents were removed using a rotary evaporator. The pNP-PEG-PE micelles were formed in 0.01 M HCl using water bath sonication. The micelles were separated from the unbound PEG and released pNP on a column with Sepharose CL-4B using the 0.01 M HCl as an eluent. Pooled fractions containing pNP-PEG-PE were freeze-dried, and pNP-PEG-PE was purified by RP-HPLC preparative column using methanol/0.01 M HCl (70/30, v/v) as a mobile phase. The fractions containing pNP-PEG-PE were collected, and the mobile phase was removed using a vacuum evaporator. pNP-PEG-PE was identified by NMR and TLC and stored as a powder at −20 °C.

2.5. Conjugating pNP-PEG-PE with polyarginine peptide

The coupling of R8 to the pNP-PEG-PE was performed as described in [23] with some modifications. Briefly, 20 mg of

pNP-PEG-PE was first dried from their chloroform solution with argon and then by overnight incubation under high vacuum. The resulting film was hydrated and dispersed by vortex for 5 min in the 5-mg/ml R8 solution in 0.01 M HCl, at the pNP-PEG-PE-to-R8 molar ratio of 1-to-1. To the suspension, 4 ml of Tris buffer, pH 9.0, was added, then mixed and incubated overnight at 4 °C under an argon atmosphere. Since the modified R8 becomes amphiphilic and forms micelles, these micelles were separated from the non-reacted free R8 by the overnight dialysis against distilled water at 4 °C using a Spectrum dialysis bag (MWCO of 5 kDa), after which samples were freeze-dried. R8-PEG-PE was identified by NMR and TLC and stored as a powder at −20 °C.

2.6. Preparation of R8-liposomal siRNA

Dry lipid film composed of egg PC, Ch, PEG-PE and DOTAP, was hydrated with a siRNA aqueous solution; siRNA was used in a quantity sufficient to neutralize the positive charge of DOTAP. The mixture was first heated to 50 °C for 30 min, then cooled to room temperature, and then transferred onto a dry film formed by drying the conjugate of R8-PEG-PE in methanol. The system was incubated at 37 °C incubation for another 2 h, the molar fraction of R8 conjugate being 0.5–1.0% of total lipid. To quantify the liposome-incorporated R8, the fluorescence intensity of 9,10-phenan-traquinone-labeled R8 was then determined by lysing the liposomes with 0.5% SDS and measuring fluorescence intensity at λ_{ex} 270 nm and λ_{em} 400 nm. Since the initial quantities of R8 and phospholipid were always known, as well as the number of phospholipid molecules forming a liposome of a given size [24], we could estimate the exact quantity of a given R8 associated with a single liposome. The R8 incorporation ranged from 300 to 500 molecules per liposome with the diameter of 150 nm.

2.7. Characterization of R8-liposomal siRNA

Liposomal dispersions were cryofixed by plunging into liquid ethane cooled in liquid nitrogen. Freeze-fracture replicas were prepared using a Balzers BAF 400D freeze-etching system, and the replicas were negatively stained by 1% uranyl acetate and examined with a JEOL 100 CX electron microscope. Particle size and surface charge were determined on a Zetasizer 3000 (Malvern Instruments, Malvern, UK).

To estimate the siRNA encapsulating efficiency in liposome and to examine siRNA serum stability, samples of siRNA or FITC-labeled siRNA either in aqueous solution or in different liposomal preparations were incubated at 37 °C alone or mixed in a 1-to-1 ratio with fresh mouse serum to give a 50% serum concentration. Aliquots of each sample taken at different incubation times were loaded onto a gel, and the electrophoresis was performed to visualize intact siRNA, which enters the gel and runs as a clearly visible band when stained with ethidium bromide.

## 2.8. Cellular translocation of R8-liposomal siRNA

The lung squamous cell carcinoma (SK-MES-1), non-small cell lung carcinoma (A549), and small cell lung carcinoma (NCI-H446) cell lines were purchased from American Type Culture Collection (ATCC, HTB-58, Manassas, VA). The SK-MES-1 cells were cultured in Eagle's minimal essential medium, the A549 cells and NCI-H446 cells were cultured in RPMI1640, supplemented with 10% FBS, 1.0 mM sodium pyruvate and 0.03% L-glutamine and maintained at 37 °C with 5% CO_2 in a humidified atmosphere.

Intracellular trafficking and localization of R8-liposomes were tested in vitro in all three chosen human lung cancer cell lines. After seeded in 35-mm dishes having glass cover slip bottoms (MatTek Corporation, Ashland, MA), all cells were grown to 60–70% confluency and then incubated with Rh-PE-labeled R8-liposomes or "plain" liposomes in a 10% FBS medium at 37 °C or 4 °C for 1, 3, 6 and 24 h. Thirty minutes prior to visualization, the cells were incubated with 100 μl of the Hoechst 33342 solution (2 μM in PBS) at 37 °C. Cells were washed three times with sterile PBS, mounted in PBS and covered with cover slip sealed with nail polish. The living cells were directly analyzed with a Leica TCS-SP confocal laser scanning microscope equipped with a 488-nm Argon, 568-nm Krypton, and 647-nm HeNe laser. Laser power and photo-multiplier settings were kept identical for all samples to make the results comparable.

To test whether R8 peptides were able to deliver siRNA-containing liposomes into all three different human lung cancer cell lines, the cells were seeded in 35-mm dishes having glass cover slip bottoms, grown to 60–70% confluency, and treated with FITC-siRNA-containing R8-liposomes or plain liposomes (in the quantity required to deliver 0.25 μg of RNA per 10,000 cells at siRNA concentration of 0.16 μg/μl added liposomal suspension) in serum-free, 2% FBS, 5% FBS, 10% FBS and 15% FBS media at 37 °C for 6 h. Cells were studied by confocal microscopy as described above.

2.9. Silencing HDM2 gene

SK-MES-1 cells were treated with different concentrations of R8-liposomal HDM2-siRNA for 24 h or 36 h, both adherent and floating cells were collected, and then PT-PCR and Western blot analysis were performed. For Western blot, centrifuged lysates (30 μg of protein) from each sample were analyzed by 10% SDS-polyacrylamide gel electrophoresis and transferred to a polyvinylidene difluoride (PVDF) membrane by semi-dry transfer. The membranes were blocked for 1 h at room temperature in Tris-buffered saline containing 0.1% Tween 20 and 3% BSA. Blots were probed with the following primary monoclonal antibodies overnight at 4 °C: anti-HDM2 and anti-β-actin antibodies (Santa Cruz Biotechnology Inc., Santa Cruz, CA, USA), This was followed by incubation with the appropriate horseradish peroxidase-conjugated secondary antibody at a dilution of 1:1000 for 1 h. Detection was achieved by enhanced chemiluminescence (Amersham Pharmacia Biotech) and exposed to film. Filters were quantitated by scanning
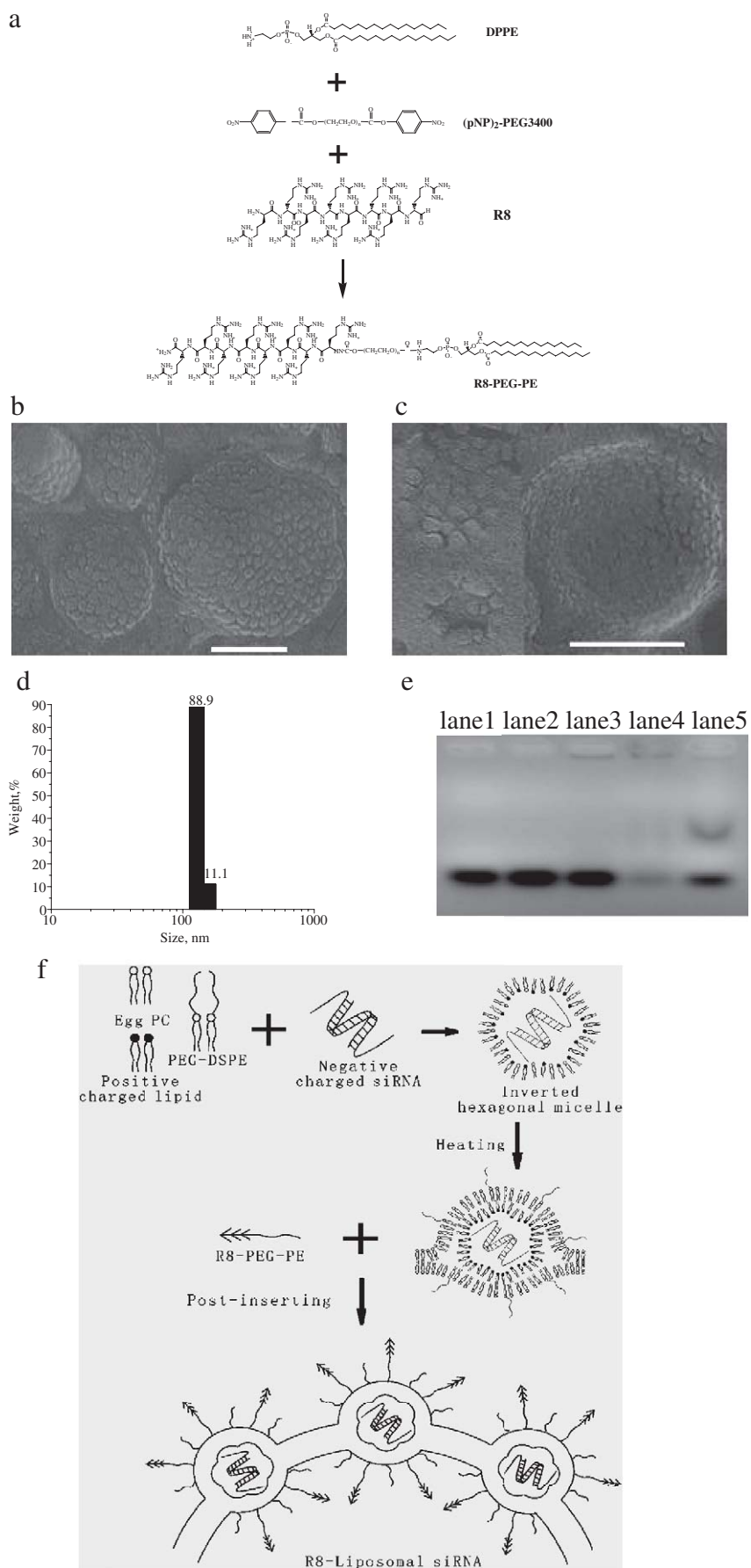
densitometry using a Bio-Rad model 620Video Densitometer with a 1-d Analyst software package for Macintosh.

Total RNAs were prepared from culture cells (1×10^6) transfected with different concentrations of R8-liposomal HDM2-siRNA for 24 h. PT-PCR was carried out using a SuperScipt™ One-Step RT-PCR kit (Invitrogen, Catalogue No. 10928-034). Oligonucleotide primers used are as follows: HDM2 Forward, 5′-AGGGAAGAAACCCAAGACA-3′; HDM2 Reverse, 5′-AGGCTGAGGCAGGAGAATG-3′; β-actin Forward, 5′-CCCAGGCACCAGGGCGTGATGGT-3′; β-actin Reverse, 5′-GGACTCCATGCCCAGGAAGGAA-3′. β-Actin mRNA was used as internal control. Amplification products were resolved by agarose gel electrophoresis and visualized by ethidium bromide staining.

2.10. Growth inhibition of tumor cells

SK-MES-1 cells were seeded in 96-well tissue culture microtiter plates. After 24 h, the culture medium was removed, and the cells were treated with R8-liposomes, R8-lipo-HDM2 siRNA, or R8-lipo-Mock siRNA in 10% FBS medium. The experiments were carried out with or without siRNA at several different concentrations of R8-liposomes and R8-lipo-siRNA provided siRNA concentrations from 50, 100 to 200 nM. After 24 h and/or 48 h, Cell-Titer 96 Aqueous One solution (Promega) was added to each well, and the plates were incubated for 4 h. This assay is based on the bioreduction of 4, 5 dimethythiazol-3-carboxymethoxy-phenyl-4-sulfophenyl-tetra-zolium compound (MTS) into a colored soluble formazan product. The viability of cells was measured using a plate reader (Thermo, Germany) at 490 nm. Relative viability was calculated with cells treated with medium alone as control. The statistical analysis of the data was performed according to the Student's *t*-test for two populations.

3. Results

3.1. siRNA-containing R8-liposomes

We have developed a simple method for producing siRNA-containing R8-liposomes (R8-lipo-siRNA). The method involves the hydration of a dry lipid film composed of 60 mol % egg PC, 34 mol% Ch, 3 mol% PEG-PE), and 3 mol% DOTAP, with DEPC-treated aqueous solution of the siRNA, in which siRNA concentration was chosen such as to neutralize the positive charge of DOTAP (zeta potential of the final preparation should be around zero). Then, siRNA-containing liposomes were incubated with the conjugate of R8 with pNP-PEG-PE. The final formulation contained a sterically protecting layer of PEG and exposed moieties of cell-penetrating peptide R8, which should allow for the efficient delivery of the liposomal siRNA into cells. See related schemes in Fig. 1. Zeta potential values of all liposomal preparations measured using a Zetasizer 3000 demonstrated that both, liposome without R8 attachment and liposomes with R8 (0.5% molar ratio) attachment had positive zeta potentials, 3.6 ± 1.2 and 5.5 ± 1.7, respectively. When the same quantity of siRNA was encapsulated in these liposomal preparations, the zeta potential of liposomes without R8 attachment was around zero (0 ± 1.0). The liposomes with attached R8 had insignificant increase in the zeta potential value to 0.5 ± 0.7.

The structures of the preparations made as above were characterized by the freeze-fracture and negative stain electron microscopy (EM). R8-lipo-siRNA particles appear nearly round with numerous tiny spherical formations tightly adhered to each other and forming a mosaic pattern on the particle surface, these formations having the size around 20 nm (Fig. 1b). The cross-fractures through the particles revealed that the particles were hollow and had a similar organization on both outer and inner sides (Fig. 1c). Particle size was in the range of 50–200 nm, this result being consistent with the data obtained using the dynamic light scattering analysis (Fig. 1d). Shape and size of the resulting particles were also confirmed by the negative stain EM (data not shown). Interestingly, the structure of siRNA-containing R8-liposomes resembles the structure of the SARS coronavirus [25], although the relevance and significance of this finding remains unclear.

Where are the molecules of siRNA located, inside the small particles or in the hollow core of the lager particle? To address this question, gel-electrophoresis was used to determine the trace of siRNA. Two different dispersions were prepared with the same quantity of siRNA and lipids. One preparation was obtained as described above (R8-lipo-siRNA), while the other was obtained by mixing pre-formed cationic R8-liposomes with siRNA aqueous solution and termed R8-liposome-siRNA complex (Comp-R8-lipo-siRNA). Samples containing the same quantity of siRNA were loaded onto the gel, and electrophoresis performed with further visualization of siRNA bands by staining with ethidium bromide (Fig. 1e). In case of Comp-R8-lipo-siRNA, all siRNA was released in a free form, resulting in a band with intensity close to the control-free siRNA (Fig. 1e, compare lanes 2 and 3). For R8-lipo-siRNA, a band with much lower intensity compared to the control free siRNA was seen, however, after the treatment of the preparation with 0.5% sodium dodecyl sulfate (SDS) for 10 min at 37 °C, two siRNA bands were seen with intensity markedly brighter than before lysing (Fig. 1e, compare lanes 2, 4 and 5), one band close to the loading position with much lower intensity compared to another one with intensity and position close to the control free siRNA. In addition, siRNA in the R8-lipo-siRNA preparations cannot be stained by ethidium bromide, suggesting that siRNA molecules were tightly coated by lipid membrane [26].

Fig. 1. Formation, characterization and assembly mechanism of R8-lipo-siRNA. (a) Synthetic scheme for intracellular chemical conjugate between an octamer of L-arginine and pNP-PEG-DPPE (R8-PEG-PE) by coupling pNP-PEG-PE to amino group of R8 molecule with the formation of a stable carbamate. (b) Freeze-fracture EM of R8-lipo-siRNAs. (c) Freeze-fracture EM of cross-fracture through R8-lipo-siRNAs. (d) Size distribution pattern of R8-lipo-siRNAs measured by dynamic light scattering. (e) Gel-electrophoresis results of mock (lane 1), free-siRNAs (lane 2), Comp-R8-lipo-siRNA (lane 3), R8-lipo-siRNA (lane 4) and 0.5% SDS treated R8-lipo-siRNAs (lane 5). (f) Schematic of the siRNA encapsulation in a small particle and assembly a large particle.

Based on the previous data [27,28] and information presented here, we proposed the following mechanism for the assembly of R8-lipo-siRNA (Fig. 1f). When the positively charged dry lipid film is hydrated with the aqueous solution containing 21 nt short double-stranded and strongly negatively charged RNA, two types of different forces act within the system: (1) electrostatic interaction between siRNA and the cationic polar heads of DOTAP drives the formation of inverted hexagonal structures entrapping single siRNA molecule, and (2) hydrophobic interaction between lipids resulting in the formation of a bilayered liposomal membrane, with PEG-PE preventing vesicles from aggregation. Heating the system induces the rearrangement of the lipid molecules and membranes to cover the surface of small inverted hexagonal micelles and arrange them to form a larger mosaic vesicle. A theoretical calculation further supports the above model. 21 nt siRNA can be considered as a rigid rod, 44 Å in diameter and 72 Å in length. The thickness of the lipid bilayer in egg PC vesicles is about 5–10 nm and varies with the acyl chain length [29]. The freeze-fracture EM shows that a small vesicle has a diameter of about 20 nm in diameter, indicating that the small vesicle represents a single siRNA molecule coated by a single lipid bilayer.

3.2. Stability of siRNA in R8-liposomes

Since the exonucleolytic degradation is the main mechanism for siRNA degradation in serum, we investigated whether the siRNA in the structure of R8-lipo-siRNA is protected from such

degradation. The results demonstrate that the incubation of the free siRNA and FITC-labeled siRNA with serum resulted in their degradation, and, after 6 h, the siRNA was fully degraded (Fig. 2a and b), while on the picture for R8-lipo-siRNA incubated with 50% serum for various time intervals only the control band can be seen (Fig 2c). After R8-lipo-siRNA lysis by SDS, however, the loaded siRNA was released from the liposomes, and all bands were seen with the intensity close to that of the control free siRNA except the mobility of all bands was slower than that of the free siRNA (Fig. 2d). The fact that siRNA released from R8-lipo-siRNA by SDS had a slower mobility than free siRNA could be explained by possible interaction of SDS and serum components with siRNA released from R8-lipo-siRNA. Size exclusion and electrostatic interaction are main factors retarding the mobility of the released siRNA from R8-lipo-siRNA.

The siRNAs encapsulated in R8-liposomes showed a very high stability in serum and remained intact even after 24-h incubation. At the same time, traditional cationic lipoplexes, such as Lipofectamine2000 and DOTAP, cannot protect siRNA from serum-mediated degradation for longer times yielding the product just a little more stable than the naked siRNA (notice the presence of siRNA degradation products in Fig. 2e and f). It is possible that siRNA cannot condense into the complexes formed by Lipofectamine2000 and DOTAP and remain exposed for degradation. When these complexes were subjected to electrophoresis, all siRNAs were released in their free form, resulting in a band with intensity close to the control free siRNA (Fig. 2g, compare lanes 1, 3 and 4).
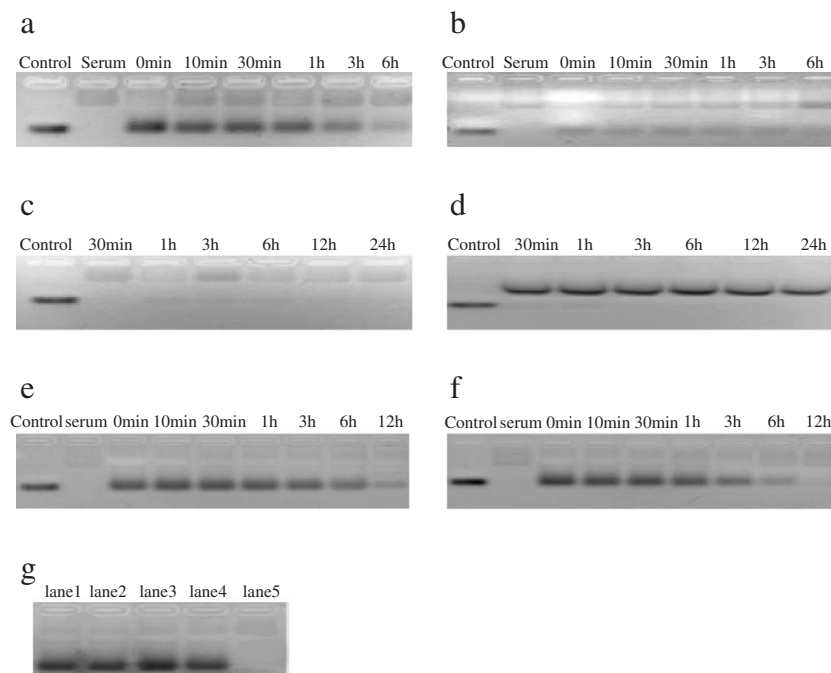

Fig. 2. Serum stability of siRNA in different lipid preparations and FITC labeled siRNA. (a) Free-siRNAs, (b) FITC labeled siRNA, (c) R8-lipo-siRNAs and (d) the samples from (c) treated by 0.5% SDS at 37 °C for 10 min, (e) Lipofectamine2000-siRNA complex prepared according to manufacturer's procedure with positive charge excess (+15±2.3), (f) DOTAP-siRNA complex prepared by hydration of DOTAP film with a siRNA solution at charge ratios (DOTAP/siRNA) of 5-to-1, (g) free-siRNAs (lane 1), FITC labeled siRNA (lane 2), Lipofectamine2000-siRNA complex (lane 3), DOTAP-siRNA complex (lane 4), R8-lipo-siRNA (lane 5) were untreated with 50% mouse serum.

3.3. Translocation of R8-lipo-siRNA into cancer cells

To test the translocation efficiency of R8-liposomes and the dependence of their cellular uptake and distribution on time and temperature, liposomes with and without R8 were labeled with Rh-PE. The process of their uptake and distribution was visualized by confocal microscopy in three lung cancer cell lines. The uptake and distribution of R8-liposomes were similar in all cell types (Fig. 3a). Typical patterns of time-dependent translocation of R8-liposomes are shown for SK-MES-1 cells. As shown in Fig. 3b, cell nuclei were stained blue with Hoechst 33342; after 1 h, an overlay shows no evidence of co-localization of R8-liposome labeled with Rh-PE with Hoechst 33342, indicating that R8-liposomes accumulated predominantly at the cell membrane and/or cytoplasm. With time, R8-liposomes, similar to TAT-liposomes [20], gradually migrate closer to nuclei, and after 3 and 6 h, a significant fraction of R8-liposomes was seen within the perinuclear region (Fig. 3b). There was virtually no uptake of liposomes without R8 by any cell type even upon the incubation for as long as 24 h (data not shown).

The effect of the temperature on the uptake process was examined following the incubation of fluorescently labeled R8-liposomes with cells at 4 °C for various times. As shown in Fig. 3c, R8-liposome-associated fluorescence was observed only at the plasma membrane of cells. With time, the fluorescence intensity was increased, but still remained accumulated on the plasma membrane. These data suggest that R8-mediated liposome uptake by cells proceeds via an active temperature-dependent mechanism rather than by direct penetration across the plasma membrane of the cells [30,31].

Can siRNA be delivered into different types of cells by R8-liposomes? To address this question, the HDM2-siRNA was labeled with FITC to observe the translocation of siRNA by confocal microscopy. In our experiments, we compared the transfection efficacy with liposomes with and without attached R8. R8-lipo-siRNA demonstrated an efficient transfection in all three types of cells even after the incubation as short as for 1 h (Fig. 4a). Liposomes without R8 modification were virtually ineffective in the delivery of siRNA into the all three types of cells even after prolonged incubation for 24 h, and no fluorescence were observed in these samples (Fig. 4b). The effect of R8-liposome on the localization of FITC-siRNA was assessed after 4 h transfection, and siRNA-associated fluorescence was observed in both of cytoplasm and nuclei.

3.4. Serum effects on R8-mediated translocation of siRNA-containing liposomes

To test serum effects on the translocation of HDM2-siRNA into A549 cells by R8-liposomes, various concentrations of the FBS were used in the culture medium. As shown in Fig. 5, after 4-h treatment, even in 10% serum HDM2-siRNA-containing R8-liposomes demonstrated a substantially higher fluorescence. Compared to the low serum-containing
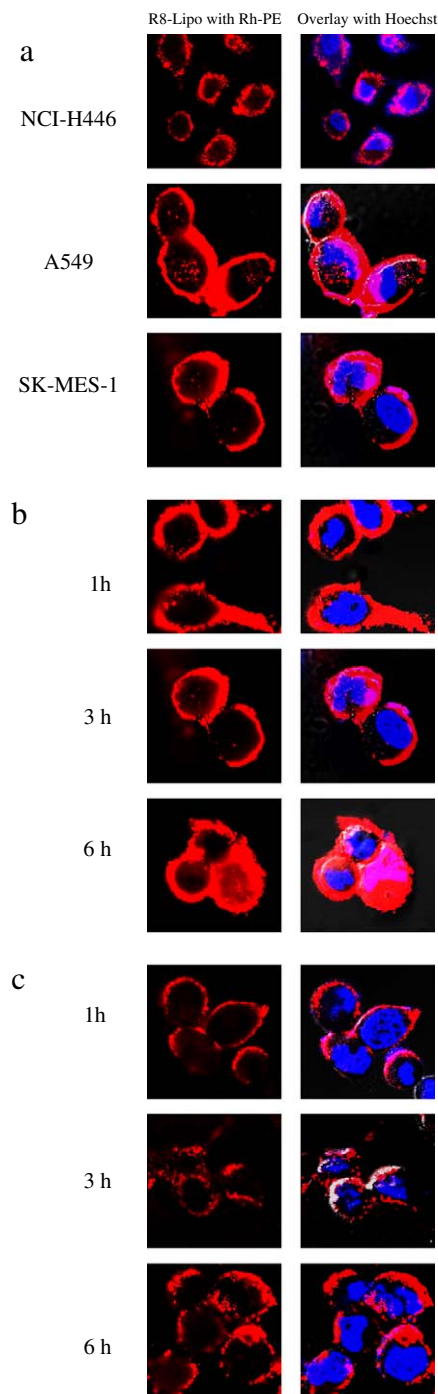

Fig. 3. Translocation of R8-liposomes. Translocation of R8-liposomes was monitored by Leica confocal microscope. Overlay images of both liposomal labels and nucleus (Hoechst 33342) were show here. The cells were treated with the same lipid concentrations (20 μg/ml) of R8-liposomes labeled with 0.1% molar ratio of Rh-PE (Red) in the medium containing 10% FBS at various temperatures for various times and subjected to Hoechst 33342 (Blue) staining. (a) All three lung cancer cells (NCI-H446, A549 and SK-MES-1) were treated with R8-liposomes at 37 °C for 3 h. (b) SK-MES-1 cells were treated with R8-liposomes at 37 °C for 1 h, 3 h and 6 h. (c) SK-MES-1 cells were treated with R8-liposomes at 4 °C for 1 h, 3 h and 6 h.

medium, 10% FBS resulted in slight decrease of fluorescence intensity in the cells treated with R8-liposomes. However, an increase in FBS concentration in the medium to above 15%
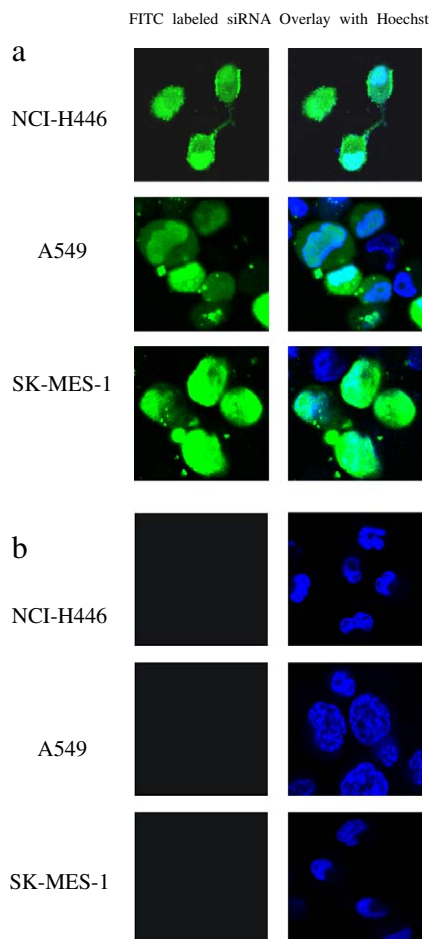
FITC labeled siRNA Overlay with Hoechst

Fig. 4. Translocation of a FITC labeled HDM2-siRNA into lung cancer cells using R8-liposome. The cells were incubation with either R8-liposome (20 µg/ml) or liposome without R8 (20 µg/ml) and fluorescent HDM2-siRN (200 nM) at 37 °C for 4 h without FBS. Overlay images of both siRNA labels (Green) and nucleus (Hoechst 33342, Blue) were monitored by Leica confocal microscope. (a) All three lung cancer cells (NCI-H446, A549 and SK-MES-1) were treated with R8-lipo-siRNA. (b) All three lung cancer cells were treated with lipo-siRNA without R8.

caused a significant decrease in R8-liposome-mediated delivery.

3.5. Bioactivity of HDM2-siRNA in R8-liposomes

The primary measure of HDM2-siRNA-mediated effects is the silencing of the target mRNA, which should result in the corresponding reduction in HDM2 protein levels. To test the silencing of HDM2 mRNA, we have used the RT-PCR method to determine HDM2-mRNA in SK-MES-1 cells. As shown in Fig. 6a, HDM2-mRNA levels were markedly down-regulated in SK-MES-1 cells transfected with R8-lipo-HDM2-siRNA in a dose-dependent manner after 24 h. Western blotting was used to examine the effects of R8-lipo-HDM2-siRNA treatment on the levels of HDM2 protein. As shown in Fig. 6b, the transfection of siRNA directed against HDM2-mRNA resulted in significant decrease in HDM2 protein levels in a dose-dependent manner after 24 h. In contrast, the expression of neither HDM2-mRNA nor

HDM2 protein was changed when the cells were treated using different concentrations of HDM2-siRNA with Lipofectamine2000, from 50 to 100, 200, and 300 nM, for various times from 24 h to 48 h (data not shown). These results suggest that R8-liposomes could provide a novel and effective way to enhance the transfection efficiency of siRNA in the presence of serum.

3.6. Toxicity of R8-liposome

The MTS method was used to examine the possible cytotoxicity of R8-liposomes in SK-MES-1 cells. After 24-h incubation with 70 µg/ml lipids, R8-liposomes killed only $14.8 \pm 3.2\%$ cells; the same quantity of Lipofectamine2000 used for comparison kills $41.3 \pm 4.7\%$ cells (Fig. 7a). Upon the extended incubation during 48 h, Lipofectamine2000 showed a high toxicity to cells with only $8 \pm 3.1\%$ survival rate (lipid concentration of 35 µg/ml). In contrast, at the same lipid concentration, after 48 h with R8-liposomes, $75 \pm 2.4\%$ cells were viable (Fig. 7b). The results show that the used concentrations of R8-liposomes were nontoxic even after 48-h incubation.

3.7. Inhibition of lung tumor cell proliferation by HDM2-siRNA in R8-liposomes

The effect of HDM2-siRNA in R8-liposomes on growth inhibition of SK-MES-1 cells was also investigated. For comparison, the cells were treated with various concentrations of R8-lipo-mock siRNA for 24 h. R8-lipo-mock siRNA did
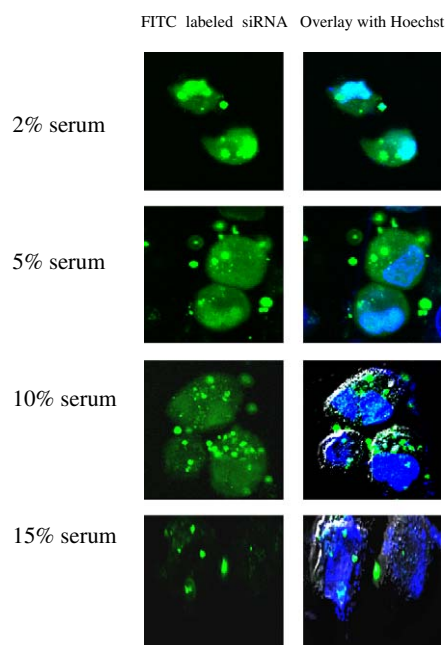
FITC labeled siRNA Overlay with Hoechst

Fig. 5. Serum effects on R8-mediated translocation of R8-lipo-siRNA into A549 cells. The cells were incubated with R8-liposome (20 µg/ml) containing fluorescent HDM2-siRN (200 nM) at 37 °C for 4 h with 2%, 5%, 10% and 15% FBS. Overlay images of both siRNA labels (Green) and nucleus (Hoechst 33342, Blue) were monitored by Leica confocal microscope.
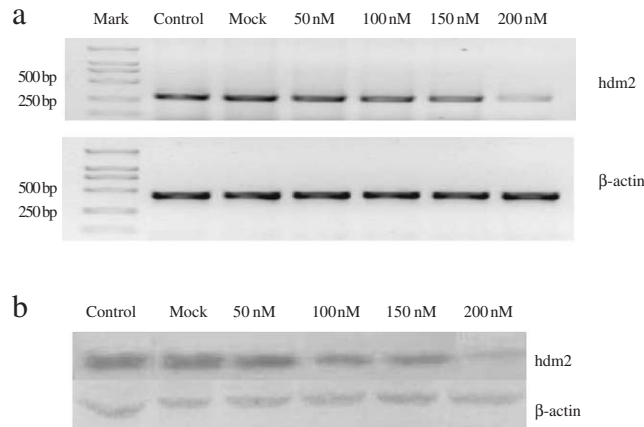
Fig. 6. HDM2-siRNA reduces expression of HDM2 gene in SK-MES-1 cells. The cells were treated with the various concentrations of HDM2-siRNA in R8-liposomes, and the expression levels of HDM2 were examined by the RT-PCR and Western bolt. (a) HDM2-mRNA levels in the cells treated with 200 nM mock siRNA (lane 3) and HDM2-siRNA different concentrations (lanes 4–7, corresponding 50–200 nM) for 24 h, untreated cells as a control (lane 2). β-Actin was used as a loading control. (b) HDM2 protein levels in the cells treated with 200 nM mock siRNA (lane 2) and HDM2-siRNA deferent concentrations (lanes 3–6, corresponding 50–200 nM) for 24 h, untreated cells as a control (lane 1). β-Actin was used as a loading control.

not inhibit the growth of tumor cells even at 200 nM siRNA (Fig. 8). However, tumor cells treated with only 100 nM of R8-lipo-HDM2 siRNA demonstrated a significant tumor cell growth inhibition ($31.2 \pm 3.6\%$ cell viability vs. $89 \pm 3.5\%$ in the presence of the same concentration of empty R8-liposomes, Fig. 8). No toxicity was observed, when the cells were treated with the naked HDM2-siRNA even at a concentration as high as 500 nM. These results clearly confirm that the therapeutic activity of siRNA can be significantly enhanced by using the nontoxic and serum-resistant R8-liposomes.

4. Discussion

The R8-liposomes loaded with HDM2-siRNA demonstrated a high stability and protected the incorporated siRNA from the degradation by the blood serum even after 24-h incubation. This system allows for very high transfection efficiency in all
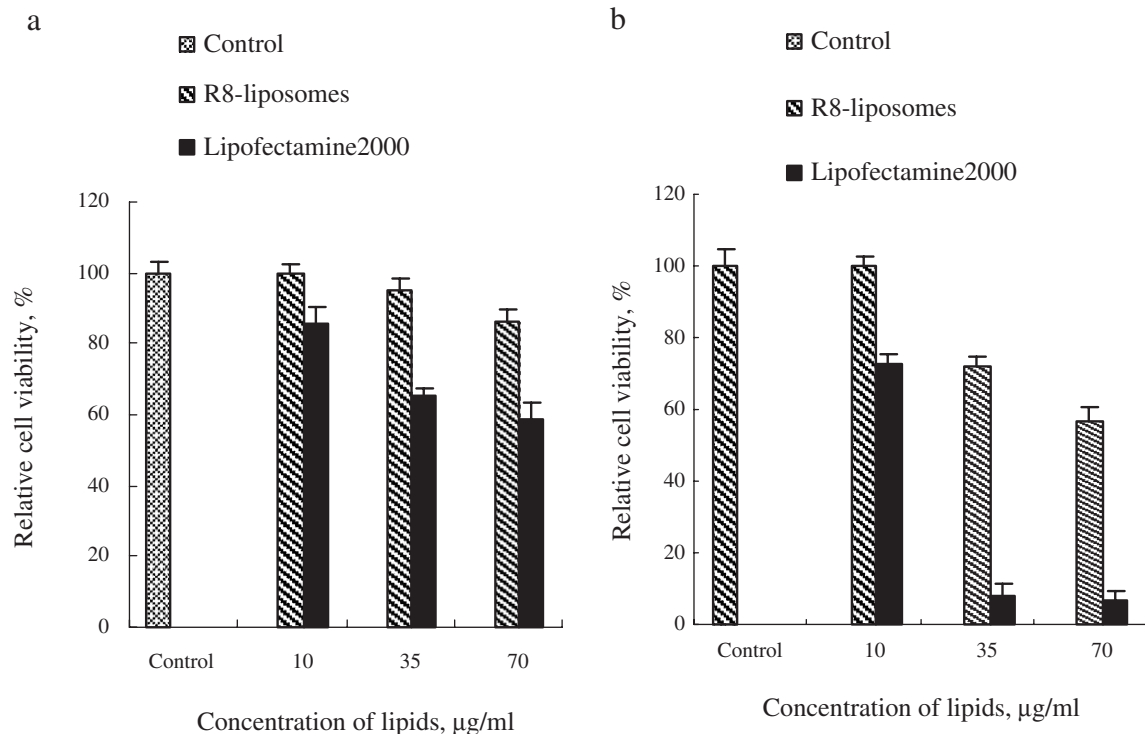

Fig. 7. Toxicity of R8-liposome. Comparative cytotoxicity of R8-liposome and Lipofectamine2000 toward SK-MES-1 cells at different lipid concentrations (μg/ml) for either 24-h (a) or 48-h (b) incubation was tested. Cell viability in R8-liposomes-free or Lipofectamine2000-free medium was taken as control (100%).
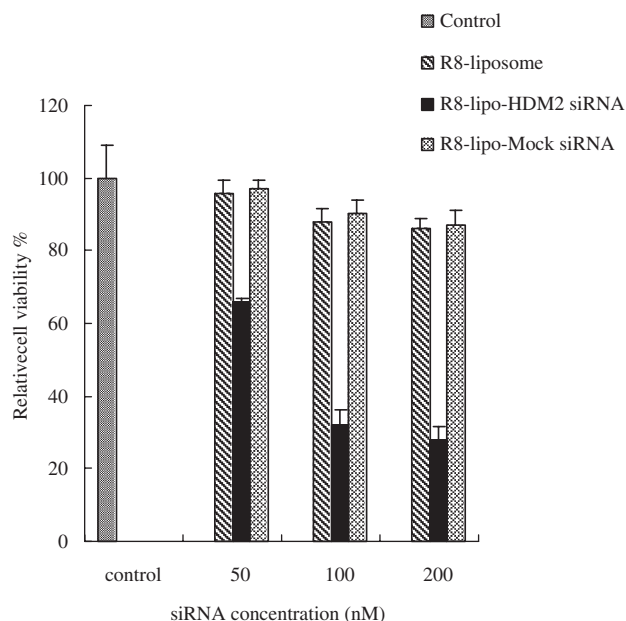
GENE DELIVERY

Fig. 8. Effect of HDM2-siRNA in R8-liposomes on the growth inhibition of SK-MES-1 cells. Cells were treated using R8-lipo-HDM2-siRNA and R8-lipo-mock siRNA, where the siRNA concentrations varied from 50 to 100 and 200 nM, the corresponding lipid concentrations were from 7.5 to 15 and 30 µg/ml. Cell viability in R8-liposomes-free medium was taken as 100%.

three types of tested lung tumor cells. The R8-liposome-mediated transfection takes place even in the presence of plasma proteins. In addition, the system has a very low cytotoxicity.

The HDM2-siRNAs-containing R8-liposomes were stable upon storage at 4 °C with less than 10% release of siRNA after 3 months (data no shown). Gel electrophoresis demonstrated that electrophoretic behaviors of R8-lipo-siRNA were significantly different from the free siRNA and the Comp-R8-lipo-siRNA (Fig. 1e), with much lower intensity compared to the free siRNA before lysing, however, after SDS lysing, two siRNA bands were seen with intensity markedly brighter than before lysing (Fig. 1e), indicating that in this case most loaded siRNA was released in a free form. The new band close to the loading position should have a higher molecular weight than free siRNA or a lesser negative charge than free siRNA, which could reflect a complex of siRNA with few DOTAP molecules formed as a result of non-complete liposome degradation by SDS or even a triple complex of negatively charged siRNA and SDS with DOTAP, since negatively charged SDS can form complexes with cationic lipids such as DOTAP in aqueous solutions. Lipid composition, size distribution, and surface charge of such liposomes can be easily manipulated to provide a clinically acceptable formulation for systemic delivery. In the process of formation of these liposomes, siRNA reacts with the head group of the liposomal DOTAP forming a neutral coordination complex. As a result, R8-lipo-siRNA have no or minimal charge. The reduction of the membrane surface charge is essential for improving the stability of siRNA-lipid formulations in the blood stream and decreasing the uptake by the reticulo-endothelial system [10]. In our study, we have

confirmed that the mechanism of action of R8-liposome-encapsulated siRNA is determined by the RNAi-mediated degradation of the target mRNA. R8-lipo-HDM2-siRNA showed biological activity in SK-MES-1 cells, demonstrating the advantages of R8-liposome encapsulation of siRNA.

The major limitations of the lipid formulations of siRNA used so far appear to be their excessive positive charge and limitation to specific cell types, which resulted in unwanted tissue distribution and high toxicity in vivo. The use of R8-liposomes as siRNA carriers is expected to overcome these problems by achieving three major goals: reduction of systemic toxicity, enhancement of the stability and circulation time of siRNA preparations in blood stream, and increase of siRNA permeation into cells. The same methodology may also prove to be useful for the encapsulation and delivery of other oligonucleotides.

R8-liposomal siRNA represent a novel non-viral preparation for applying the RNAi technique. Compared to other non-viral vectors, R8-lipo-siRNA provides an efficient silencing of the target gene, great reduction in toxicity, and high stability in serum.

References

[1] C.D. Novina, P.A. Sharp, The RNAi revolution, Nature 430 (2004) 161–164.
[2] J. Elmen, H. Thonberg, K. Ljungberg, M. Frieden, M. Westergaard, Y. Xu, B. Wahren, Z. Liang, H. Orum, T. Koch, C. Wahlestedt, Locked nucleic acid (LNA) mediated improvements in siRNA stability and functionality, Nucleic Acids Res. 33 (2005) 439–447.
[3] Y.L. Chiu, A. Ali, C.Y. Chu, H. Cao, T.M. Rana, Visualizing a correlation between siRNA localization, cellular uptake, and RNAi in living cells, Chem. Biol. 11 (2004) 1165–1175.
[4] J. Soutschek, A. Akinc, B. Bramlage, K. Charisse, R. Constien, M. Donoghue, S. Elbashir, A. Geick, P. Hadwiger, J. Harborth, M. John, V. Kesavan, G. Lavine, R.K. Pandey, T. Racie, K.G. Rajeev, I. Rohl, I. Toudjarska, G. Wang, S. Wuschko, D. Bumcrot, V. Koteliansky, S. Limmer, M. Manoharan, H.P. Vornlocher, Therapeutic silencing of an endogenous gene by systemic administration of modified siRNAs, Nature 432 (2004) 173–1788.
[5] R.M. Schiffelers, A. Ansari, J. Xu, Q. Zhou, Q. Tang, G. Storm, G. Molema, P.Y. Lu, P.V. Scaria, M.C. Woodle, Cancer siRNA therapy by tumor selective delivery with ligand-targeted sterically stabilized nano-particle, Nucleic Acids Res. 32 (2004) e149.
[6] N. Unnamalai, B.G. Kang, W.S. Lee, Cationic oligopeptide-mediated delivery of dsRNA for post-transcriptional gene silencing in plant cells, FEBS Lett. 566 (2004) 307–310.
[7] M. Lewin, N. Carlesso, C.H. Tung, X.W. Tang, D. Cory, D.T. Scadden, R. Weissleder, Tat peptide-derivatized magnetic nanoparticles allow in vivo tracking and recovery of progenitor cells, Nat. Biotechnol. 18 (2000) 410–414.
[8] V.P. Torchilin, R. Rammohan, V. Weissig, T.S. Levchenko, TAT peptide on the surface of liposomes affords their efficient intracellular delivery even at low temperature and in the presence of metabolic inhibitors, Proc. Natl. Acad. Sci. U. S. A. 98 (2001) 8786–8791.
[9] S.R. Schwarze, A. Ho, S.F.A. Vocero-Akbani, In vivo protein transduction: delivery of a biologically active protein into the mouse, Science 285 (1999) 1569–1572.

[10] A. Sharma, U.S. Sharma, Liposomes in drug delivery: progress and limitations, Int. J. Pharm. 154 (1997) 123–140.

[11] Z. Ma, J. Li, F. He, A. Wilson, B. Pitt, S. Li, Cationic lipids enhance siRNA-mediated interferon response in mice, Biochem. Biophys. Res. Commun. 330 (2005) 755–759.

[12] S. Spagnou, A.D. Miller, M. Keller, Lipidic carriers of siRNA: differences in the formulation, cellular uptake, and delivery with plasmid DNA, Biochemistry 43 (2004) 13348–13356.

[13] M. Sioud, D.R. Sorensen, Cationic liposome-mediated delivery of siRNAs in adult mice, Biochem. Biophys. Res. Commun. 312 (2003) 1220–1225.

[14] B. Dalby, S. Cates, A. Harris, E.C. Ohki, M.L. Tilkins, P.J. Price, V.C. Ciccarone, Advanced transfection with Lipofectamine 2000 reagent: primary neurons, siRNA, and high-throughput applications, Methods 33 (2004) 95–103.

[15] R.M. Brazas, J.E. Hagstrom, Delivery of small interfering RNA to mammalian cells in culture by using cationic lipid/polymer-based transfection reagents, Methods Enzymol. 392 (2005) 112–124.

[16] E.C. Ohki, M.L. Tilkins, V.C. Ciccarone, P.J. Price, Improving the transfection efficiency of post-mitotic neurons, J. Neurosci. Methods 112 (2001) 95–99.

[17] C. Lorenz, P. Hadwiger, M. John, H.P. Vornlocher, C. Unverzagt, Steroid and lipid conjugates of siRNAs to enhance cellular uptake and gene silencing in liver cells, Bioorg. Med. Chem. Lett. 14 (2004) 4975–4977.

[18] E. Vives, P. Brodin, B. Lebleu, A truncated HIV-1 Tat protein basic domain rapidly translocates through the plasma membrane and accumulates in the cell nucleus, J. Biol. Chem. 272 (1997) 16010–16017.

[19] M. Stroh, J.P. Zimmer, D.G. Duda, T.S. Levchenko, K.S. Cohen, E.B.D.T. S. Cadden, V.P. Torchilin, M.G. Bawendi, D. Fukumura, R.K. Jain, Quantum dots spectrally distinguish multiple species within the tumor milieu in vivo, Nat. Med. 11 (2005) 678–682.

[20] V.P. Torchilin, T.S. Levchenko, R. Rammohan, N. Volodina, B. Papahadjopoulos-Sternberg, G.G. D'Souza, Cell transfection in vitro and in vivo with nontoxic TAT peptide–liposome–DNA complexes, Proc. Natl. Acad. Sci. U. S. A. 100 (2003) 1972–1977.

[21] P.A. Wender, D.J. Mitchell, K. Pattabiraman, E.T. Pelkey, L. Steinman, J. B. Rothbard, The design, synthesis, and evaluation of molecules that enable or enhance cellular uptake: peptoid molecular transporters, Proc. Natl. Acad. Sci. U. S. A. 97 (2000) 13003–13008.

[22] S. Futaki, W. Ohashi, T. Suzuki, M. Niwa, S. Tanaka, K. Ueda, H. Harashima, Y. Sugiura, Stearylated arginine-rich peptides: a new class of transfection systems, Bioconjug. Chem. 12 (2001) 1005–10011.

[23] W. Liang, T. Levchenko, B.A. Khaw, V.P. Torchilin, ATP-containing immunoliposomes specific for cardiac myosin, Curr. Drug Deliv. 1 (2004) 1–7.

[24] H.G. Enoch, P. Strittmatter, Formation and properties of 1000-A-diameter, single-bilayer phospholipid vesicles, Proc. Natl. Acad. Sci. U. S. A. 76 (1979) 145–149.

[25] Y. Lin, X. Yan, W. Cao, C. Wang, J. Feng, J. Duan, S. Xie, Probing the structure of the SARS coronavirus using scanning electron microscopy, Antivir. Ther. 9 (2004) 287–289.

[26] M.I. Angelova, N. Hristova, I. Tsoneva, DNA-induced endocytosis upon local microinjection to giant unilamellar cationic vesicles, Eur. Biophys. J. 28 (1999) 142–150.

[27] J.O. Radler, I. Koltover, T. Salditt, C.R. Safinya, Structure of DNA–cationic liposome complexes: DNA intercalation in multilamellar membranes in distinct interhelical packing regimes, Science 275 (1997) 810–814.

[28] I. Koltover, T. Salditt, J.O. Radler, C.R. Safinya, An inverted hexagonal phase of cationic liposome–DNA complexes related to DNA release and delivery, Science 281 (1998) 78–81.

[29] B.A. Lewis, D.M. Engelman, Lipid bilayer thickness varies linearly with acyl chain length in fluid phosphatidylcholine vesicles, J. Mol. Biol. 166 (1983) 211–217.

[30] J.S. Wadia, R.V. Stan, S.F. Dowdy, Transducible TAT-HA fusogenic peptide enhances escape of TAT-fusion proteins after lipid raft macro-pinocytosis, Nat. Med. 10 (2004) 310–315.

[31] M.M. Fretz, G.A. Koning, E. Mastrobattista, W. Jiskoot, G. Storm, OVCAR-3 cells internalize TAT-peptide modified liposomes by endocy-tosis, Biochim. Biophys. Acta. 1665 (2004) 48–56.